Microelectronic Engineering xxx (2011) xxx–xxx

Contents lists available at ScienceDirect

Microelectronic Engineering

journal homepage: www.elsevier.com/locate/mee

Fluorescence enhancement from plasmonic Au templates

P. Petrou [a], I. Raptis [b], S. Kakabakos [a], Th. Speliotis [c], A. Gerardino [d], N. Papanikolaou [b,*]

[a] Institute of Radioisotopes and Radiodiagnostic Products, NCSR "Demokritos", Athens 15310, Greece
[b] Institute of Microelectronics, NCSR "Demokritos", Athens 15310, Greece
[c] Institute of Materials Science, NCSR "Demokritos", Athens 15310, Greece
[d] CNR-Institute for Photonics and Nanotechnology, Rome 00156, Italy

ARTICLE INFO

Article history:
Available online xxxx

Keywords:
Fluorescence
Surface plasmons
Electron beam lithography

ABSTRACT

We have fabricated sub-quarter-micron-patterned Au templates with electron beam lithography, and studied their effect on the fluorescence intensity of immobilized, anti-rabbit IgG antibody labeled with AlexaFluor® 546. Varying the geometry of the structured surface, the plasmon resonances are tuned to match the fluorescence wavelengths and achieve significant fluorescence enhancement. Full electrodynamic simulations were used to understand the optical response and access the quality of the fabricated structures for surface plasmon excitation.

1. Introduction

Light emission properties of organic molecules and quantum dots can be tailored by properly engineering the electromagnetic environment [1]. In this respect, metal nanoparticles and nanopatterned metallic surfaces are studied intensively [2–4], since light interacts with the metallic electrons and produces very strong, sub-wavelength, light localization and drastic enhancement of the local electromagnetic (EM) field. These coupled oscillations of the EM field and the conduction electrons of the metal are called surface plasmons. Generally, surface plasmon excitation can occur in a metal–dielectric interface when the dielectric function changes sign, and is characterized by light localization at the interface. The progress in the nanofabrication methodologies has revived the study of surface plasmons, which are currently considered for sensor applications but also for wave guiding in the nanoscale. The EM field enhancements could be used for non-linear optics, surface enhanced Raman scattering, or fluorescence enhancement. Due to the importance of the field, several recent reviews have been published on the physics and applications of surface plasmons [4].

Plasmon resonance frequencies depend on the metal, on the dielectric environment, as well as the shape and size of the metallic nanoparticles [5,6]. An interesting concept is to use periodicity as an additional parameter to control the plasmon excitations. The surface plasmon microscope is already used in the study of biological reactions. However, the setup is rather complicated and requires prisms to excite the surface plasmons. In this respect it would be desirable to develop low cost systems for rapid analysis of low volume samples [7]. Plasmonic interactions give a rich and complex variety of optical properties since, for example, two metallic nanoparticles in close proximity might lead to plasmon hybridization phenomena and "photonic metamolecules" since their optical response can be explained in a way similar to molecular energy spectra. An interesting plasmonic system is the periodic array of metallic nanoparticles or nanorods that combine the plasmon tunability of the individual particles with simultaneous control of the interparticle interaction, to achieve tailored plasmon excitations [6]. Enhanced fluorescence of semiconductor core–shell CdSe/ZnS quantum dots close to periodic Ag nanoparticle arrays in direct contact with an Ag surface was recently reported [8].

Our aim is to study the influence of tailored surface plasmons in the fluorescence intensity of immobilized, labeled, biomolecules. Simple optical transmission experiments are used to detect the surface plasmon resonances. Additionally, once the optimum geometries are found, electron beam lithography can be replaced by other nanofabrication methods like nanoimprint [7] or 193 nm lithography that allows for fast and low cost fabrication of plasmonic templates.

2. Results and discussion

We have first fabricated periodic arrays of sub-quarter-micron pillars in a thin PMMA film on Si substrate using electron beam lithography. Pillars with different nominal diameters d, were arranged in a square lattice with different lattice constants a. Each patterned area is 0.5×0.5 mm^2 to allow for optical characterization. High acceleration voltage (100 kV) electron beam lithography has been performed on 230 nm thick PMMA (beam current: 3 nA; dose: 400 mC/cm^2). The patterns have been developed in a MIBK:IPA = 1:1

* Corresponding author.
E-mail address: n.papanikolaou@imel.demokritos.gr (N. Papanikolaou).

0167-9317/$ - see front matter © 2011 Elsevier B.V. All rights reserved.
doi:10.1016/j.mee.2011.02.073

solution for 30 s. The height of the PMMA pillars, after development, was approximately 150 nm. The samples were subsequently covered with 150 nm Au using sputtering. An SEM micrograph of a final structure is shown in Fig. 1, where we observe a 150 nm thin Au film over the patterned PMMA layer. Nominal parameters $d = 150$ nm, $a = 450$ nm, $d = 150$ nm, $a = 500$ nm, and $d = 200$ nm, $a = 600$ nm were used for the fabrication. The analysis of the SEM images shows that the resulted patterns have somewhat larger diameters, while there is a small deviation of the fabricated patterns from the circular shape. The measured dimensions where: $a = 450$ nm, $d = 180$ nm, $a = 500$ nm, $d = 180$ nm, $a = 600$ nm, $d = 240$ nm. The optical properties of both Au pillars as well as hole-arrays in metallic films have been studied extensively in the past. In particular similar metallic nanorod structures are reported to be more sensitive to changes in the refractive index of the environment compared to isolated nanorods that makes them useful for biosensing applications [9].

For visible frequencies the samples are opaque. The reflectance was measured with a FR-Basic visible-near infrared tool (Theta-Metrisis), the experimental setup collects light at a small light cone around the normal direction. The measured spectra are shown in the upper diagram of Fig. 2. Reflectance is normalized to the one of the flat Au surface on a Si substrate. We observe strong absorption at wavelengths depending on the geometrical parameters of the structures. Absorption is due to surface plasmon modes with

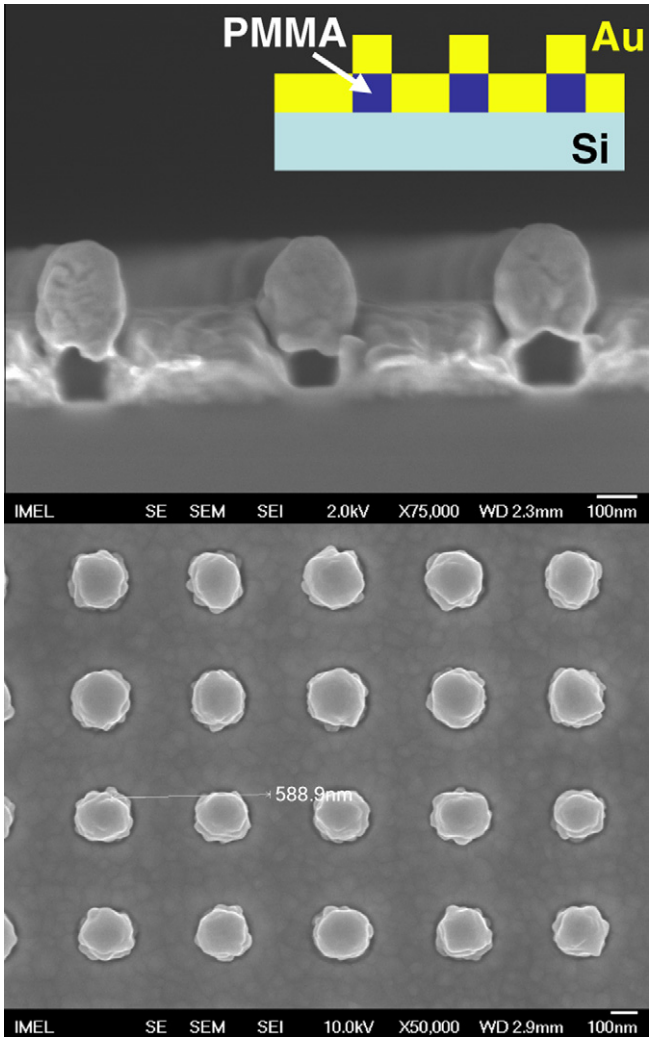

Fig. 1. Typical SEM micrographs of the patterned PMMA after sputtering with Au top: cross section and bottom: top view. In the inset, we show a schematic of the cross-section with the PMMA pillars and the Au film on top.

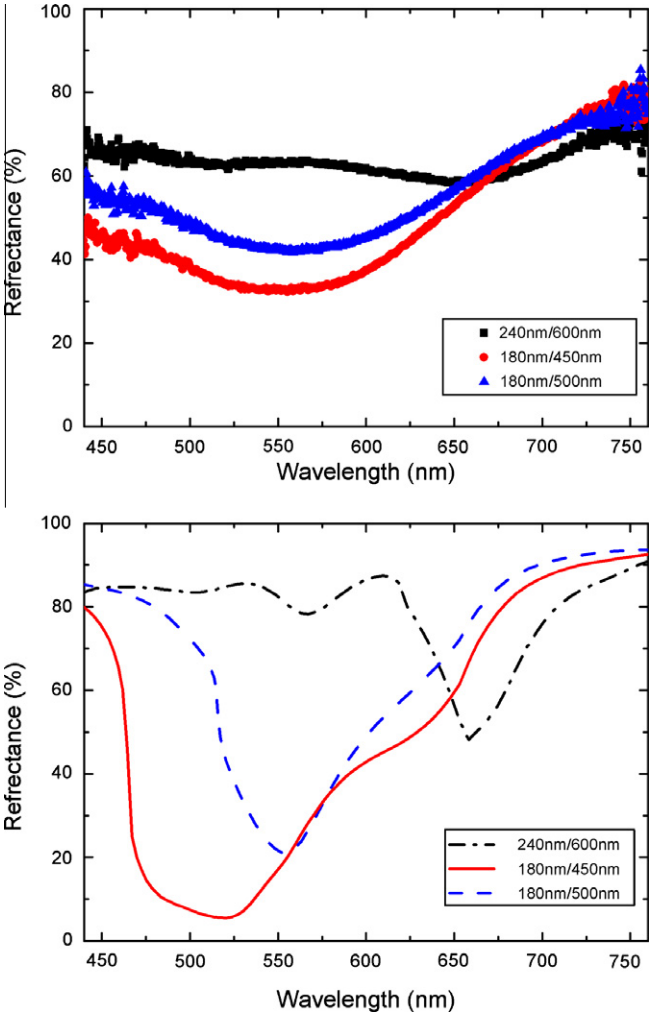

Fig. 2. Up: measured, normal incidence, reflectance spectra of Au covered PMMA pillars arranged in a square lattice with diameter $d = 180$ nm, lattice constant $a = 450$ nm triangles, $d = 180$ nm, $a = 500$ nm circles, and $d = 240$ nm, $a = 600$ nm squares. Down: simulated reflectance spectra for the same geometries, $a = 450$ nm, $d = 180$ nm full line, $a = 500$ nm, $d = 180$ nm dashed line, $a = 600$ nm, $d = 240$ nm dash-dotted line. Both theory and experiment are normalized to the reflectance of a 150 nm flat Au film on a Si substrate.

charge oscillation along the x–y plane, parallel to the surface. Plasmon modes connected with oscillations normal to the surface cannot be efficiently excited in the optical characterization setup used, since they require off-normal light incidence. The position of the resonance mainly dependents on the size of the pillars, while changing the lattice constants causes only a small shift for pillars of the same diameter. The pillars with $d = 180$ nm show strong absorption with a peak close to 560 nm wavelength while the wider $d = 240$ nm pillars have a peak in absorption around 670 nm. In order to understand the experimental spectra, we have performed full electrodynamic simulations using a multiple scattering method [10]. In our theoretical approach the structure is divided in layers that should have the same periodicity. Based on the micrographs shown in Fig. 1, we consider an 150 nm thin Au film perforated with cylindrical holes of diameter d filled with PMMA (refractive index $n = 1.5$) dielectric cylinders on an infinite Si substrate. On top of the holes we consider Au cylinders with the same diameter d and height 150 nm. Multiple scattering in each layer is calculated in a spherical basis expansion and then projected to a plane wave basis. Individual scatterers (particles or holes) are characterized by the scattering T matrix, multiple scattering events in

Please cite this article in press as: P. Petrou et al., Microelectron. Eng. (2011), doi:10.1016/j.mee.2011.02.073

the infinite periodic layers are summed using the Ewald summation method in case of a loss-less dielectric environment while direct sums converge fast for the hole arrays where losses are included in the metal [10]. The scattering from each layer is described by the scattering S matrices and multiple scattering between successive layers give us the S matrix of the whole structure. The method allows the calculation of complex geometries and the inclusion of realistic, measured, dielectric functions [11] and losses. The calculated transmission is negligibly small while the reflectance spectra, normalized to the reflectance of a flat, 150 nm thick, Au on an infinite Si substrate, are shown in the lower diagram in Fig. 2. The general trends like the red-shift of the resonance with increasing lattice constant and the relative intensities of the resonances are well reproduced, but the simulations predict stronger reflectance drops on resonance as well as higher reflectance away from the resonances. Surface roughness and small disorder in the shape of the fabricated pillars could be possible causes for this discrepancy, but also the fact that the shapes of the pillars are not exactly cylindrical as assumed in the simulation. From the simulations we conclude that the plasmon resonances observed are due to particle plasmons of the top Au pillars. Interestingly the presence of the hole-array does not give extra plasmon excitations in the visible-near infrared up to 800 nm. However, the calculations show that for different layout characteristics delocalized plasmons on the Au film can be also excited in this geometry [12]. A more detailed theoretical study of this system will be published elsewhere.

In order to evaluate the effect of Au surface nanostructuring on the fluorescence intensity of immobilized molecules, images of the patterned areas as well as of the surrounding planar Au surface were obtained using an epifluorescence microscope (Axioskop 2 Plus; Carl Zeiss), facilitated with a 8-bit digital camera, both prior to and after biomolecule immobilization, using exactly the same camera settings. Two different filter sets where used to investigate the spectral windows where surface plasmons show a resonance. We used a band-pass excitation filter at 546 nm (±12 nm) with a band-pass emission filter at 575–640 nm for the 180 nm pillars and an excitation filter at 625–655 nm with a band-pass emission filter at 665–720 nm for the 240 nm pillars. After acquisition of the images and the spectra of the untreated surfaces, a 10 mg/L solution of an anti-rabbit IgG antibody labeled with AlexaFluor® 546 (Molecular Probes, Inc., Eugene, OR, USA) diluted in phosphate buffer 50 mM, pH 7.4, was applied onto them for 1 h at room temperature. Then, the surfaces were washed extensively with phosphate buffer 50 mM, pH 7.4, and distilled water and dried under nitrogen flow. A typical image from the microscope is shown in the upper part of Fig. 3. Strong fluorescence enhancement in the pattered areas is seen in all cases. The fluorescence spectra through the microscope objective (×40), acquired with the FR-μProbe (Theta-Metrisis), are shown in the lower part of Fig. 3. For comparison, in Fig. 4 we also show the absorption and fluorescence spectra of the biomolecules in solution. All Au surfaces, both patterned and planar provided the same signal prior to labeled antibody immobilization. This signal was taken as background signal (arising mainly from the reflection of the incident light from the Au surface) and subtracted from the signals determined after the labeled antibody immobilization. The results show an increase in the fluorescence for all patterned surfaces that ranges form 30 to 70 times compared to the surrounding flat Au surface. The highest signal increase was obtained from the pattern with pillars of diameter of 180 nm and lattice constant 450 nm. This structure shows the strongest light absorption close to the emitted fluorescence wavelengths, as seen from Fig. 3. The fluorescence enhancement is reduced but still remains significant in the other patterned surfaces while stronger light absorption generally leads to bigger enhancement. As supported also by the simulations, there is significant potential to tailor the plasmon excitation by optimizing fabrication and geometry.

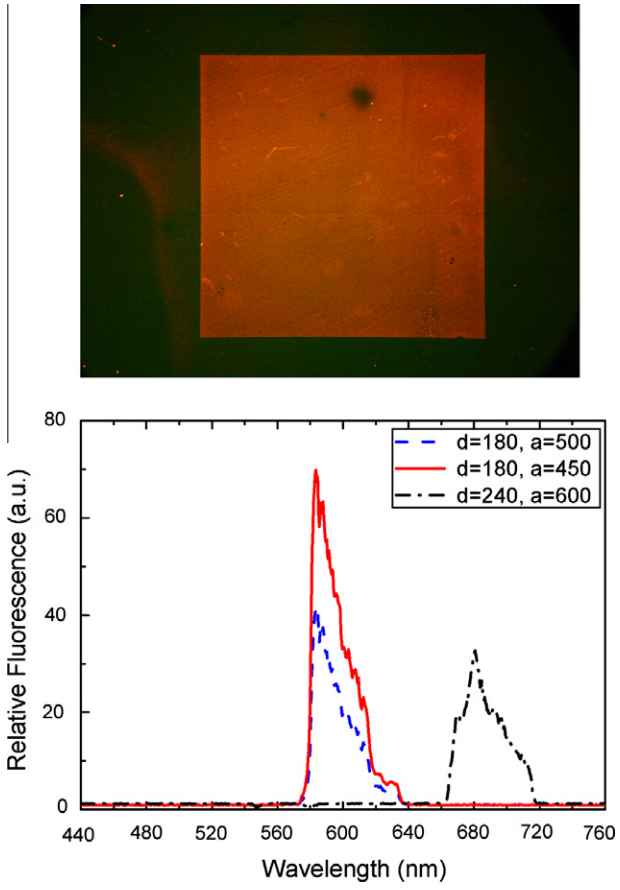

Fig. 3. Up: typical fluorescence image obtained from a patterned area $a = 450$ nm, $d = 180$ nm (bright square) surrounded by flat Au surface after coating with anti-rabbit IgG antibody labeled with AlexaFluor 546. Down: fluorescence of antibody in the three different patterned areas ($d = 180$ nm, $a = 450$ nm full line, $d = 180$ nm, $a = 500$ nm dashed line, $d = 240$ nm, $a = 600$ nm dash-dotted line) normalized by the fluorescence of the antibody on the unpatterned Au surface.

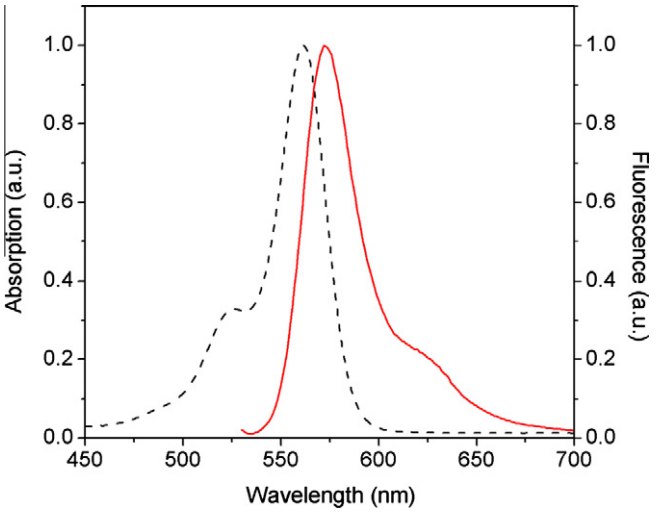

Fig. 4. Normalized absorption (black, dotted line) and emission spectrum (red, full line) of a 100 nM solution of anti-rabbit IgG antibody labeled with AlexaFluor 546 in 50 mM phosphate buffer, pH 7.4. (For interpretation of the references to colour in this figure legend, the reader is referred to the web version of this article.)

3. Conclusion

Gold covered patterned PMMA surfaces were found to enhance the fluorescence intensity of directly immobilized-fluorescently labeled biomolecules up to 70 times compared with a flat Au surface. This fluorescence signal enhancement could be beneficial in terms of increased detection sensitivity. However, the discrepancy between measured and simulated spectra requires further study. Moreover, a richer plasmon spectrum is expected for different geometries but also for off-normal incident light which should be more sensitive to changes of the refractive index and could be used for label free detection of biomolecules.

Acknowledgment

The authors would like to thank NCSR "Demokritos" for financial support of this work through project "Demoerevna" E-1437.

References

[1] E.M. Purcell, Phys. Rev. 69 (1946) 861.
[2] E. Ozbay, Science 311 (2006) 189.
[3] F.J. Garcia de Abajo, Rev. Mod. Phys. 79 (2007) 1267.
[4] (a) S.A. Maier, Plasmonics: Fundamentals and Applications, Springer, Dordrecht, 2007; (b) M.L. Brongersma, P.G. Kik, Surface Plasmon Nanophotonics, Springer Series in Optical Sciences, vol. 131, Springer, Dordrecht, 2007.
[5] Lal S. Link, N.J. Halas, Nat. Photonics 1 (2007) 641.
[6] J.N. Anker, W.P. Hall, O. Lyanders, N.C. Shah, J. Zhao, R.P. vanDuyne, Nat. Mater. 7 (2008) 442.
[7] M.E. Stewart, N.H. Mack, V. Malyarchuk, J. Soares, T.-W. Lee, S.K. Gray, R.N. Nuzzo, J.A. Rogers, PNAS 103 (2006) 17143.
[8] J.H. Song, T. Atay, S. Shi, H. Urabe, A.V. Nurmikko, Nano Lett. 5 (2005) 1557.
[9] A.V. Kabashin et al., Nat. Mater. 8 (2009) 867.
[10] N. Stefanou, V. Yannopapas, A. Modinos, Comp. Phys. Commun. 132 (2000) 189;
G. Gantzounis, N. Stefanou, Phys. Rev. B 73 (2006) 035115.
[11] E.D. Palik (Ed.), Handbook of Optical Constants of Solids, Academic, New York, 1998.
[12] T.A. Kelf et al., Phys. Rev. B 74 (2006) 245415.